



**Technical Reports**  
Volume 12, No. 4

**Trip Report for**  
**“Cambridge Healthtech Institute’s**  
**International Molecular Medicine Tri-Conference”**  
**San Francisco, California**  
**February 28 - March 2, 2007**

**Aruna Sambandam, Ph.D.**

---

**Abstract:** *Cambridge Healthtech Institute’s “Fourteenth International Molecular Medicine Tri-Conference” was held in San Francisco, CA, from February 28 – March 2, 2007. Attendees from biotech and pharmaceutical companies, as well as academia attended this conference. This symposium featured nine concurrent tracks. This report highlights select material from information presented in seminars from Track 3: Mastering Medicinal Chemistry.*

---

---

**“TRPV1 Antagonists - A Case Study – From High Throughput Screening to Human Clinical Trials,”**

*Mark H. Norman, Ph.D. (Amgen)*

The vanilloid receptor-1 (VR1) or the transient receptor potential ion channel – vanilloid receptor 1 (TRPV1) is a non-selective ion channel, highly permeable to  $\text{Ca}^{2+}$ . TRPV1 is expressed predominantly by peripheral sensory neurons and is involved in the perception of pain. TRPV1 is activated by stimuli such as heat ( $> 43\text{ }^{\circ}\text{C}$ ), pH (pH 5), and by ligands such as capsaicin, anandamide and products of lipoxygenase and is up-regulated during inflammation. Inflammatory pain models utilizing knockout mice lacking the TRPV1 gene show reduced thermal hyperalgesia; the KO mice have normal nerve structure, body weight and body core temperature. Thus, TRPV1 may constitute a target for the treatment of pain (table 1).

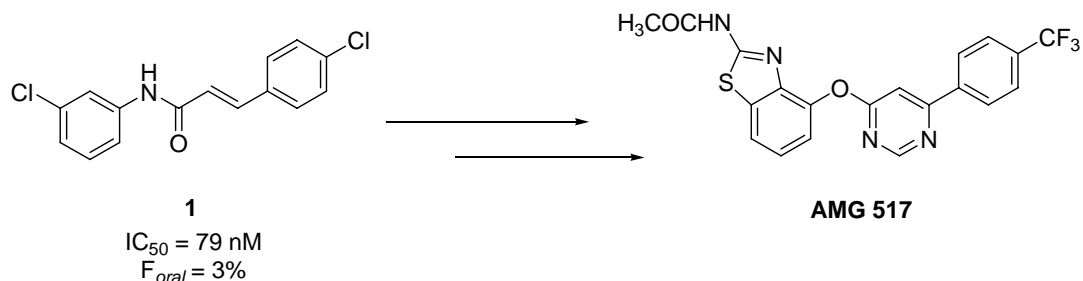
**Table 1**

**TRPV1 Expression in Human Disease**

- **Chronic Pain Patients**
  - Post-herpetic neuralgia
  - Diabetic Neuropathy
  
- **Chronic Obstructive Pulmonary Disease**
  - Asthma
  
- **Other Published Studies**
  - Visceral: Elevation of VR1 in rectal hypersensitivity and fecal urgency
  - IBD: VR1 immunoreactivity is greatly increase in colonic nerve fibers of patients with IBD
  - Bladder: Patients with neurogenic detrusor overactivity have elevated VR1 nerve fibers
  - Tooth Pulp: Dense VR1 innervation

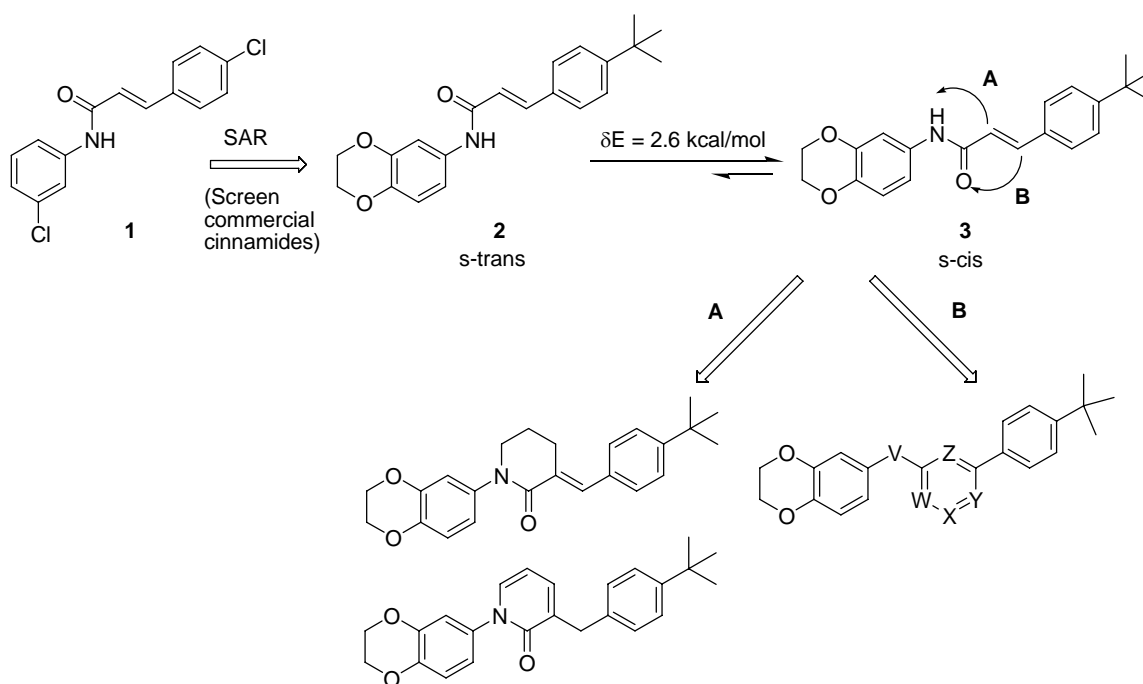
Capsaicin, an agonist of TRPV1, causes hyperstimulation of TRPV1, leading to desensitization of nociceptors to additional noxious stimuli. Capsaicin is a constituent of several topical muscle pain relievers, and has been used to treat pain associated with diabetic neuropathy and arthritis. However, the use of capsaicin as an analgesic is not devoid of side effects, including a burning sensation, irritation and neuronal damage due to continuous  $\text{Ca}^{2+}$  influx into cells. TRPV1 antagonists, on the other hand, block channel activity, and prevent neuronal firing, and have potentially fewer side effects.

Amgen scientists developed a high throughput assay to screen the approximately 1 million compounds in the Amgen library for TRPV1 antagonists (the luminescence-based assay allows for detection of agonists as well). Of the HTS hits, one, cinnamide **1**, was optimized to give the clinical candidate AMG 517.



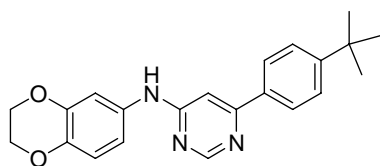
Compound **1** underwent numerous structural changes en route to AMG 517, including the introduction of conformational restriction (Figure 1).

**Figure 1**



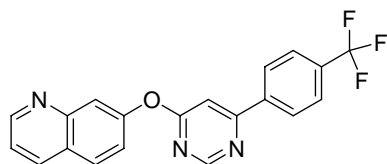
The synthesis of analogues resulting from cyclization route B yielded compound **4**, bearing a pyrimidine group. Variation of the linker revealed that an ether linkage could replace the amine linker (Table 1). Optimization of oral bioavailability was achieved by (a) replacement of the benzodioxolane group with a quinoline moiety (leading to increased potency) and (b) replacement of the *tert*-butyl group with a trifluoromethyl

group (resulting in increased metabolic stability), leading to compound **5**, with  $F_{oral} = 31\%$ .



**4**

rTRPV1 (capsaicin)  $IC_{50} = 120$  nM



**5**

rTRPV1 (capsaicin)  $IC_{50} = 7$  nM

$F_{oral} = 31\%$

**Table 1**

V	rTRPV1(Cap) $IC_{50}$ (nM)
NH	120
NMe	>4000
O	290
S	>4000
CH <sub>2</sub>	914

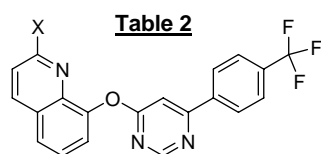
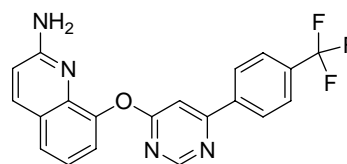


**Table 2**

X	rTRPV1(Cap) $IC_{50}$ (nM)	rTRPV1(pH5) $IC_{50}$ (nM)
OMe	>4000	>4000
NH <sub>2</sub>	11	62
NHMe	35	43
NMe <sub>2</sub>	>4000	>4000
NHAc	77	15



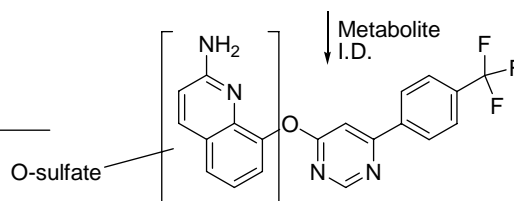
**6**

rTRPV1 (capsaicin)  $IC_{50} = 11$  nM

rTRPV1 (pH 5)  $IC_{50} = 62$  nM

$CL_{in vitro}$  (RLM) = 110  $\mu$ l/min/mg

$CL_{in vivo}$  (rat) = 1.2 L/h/kg

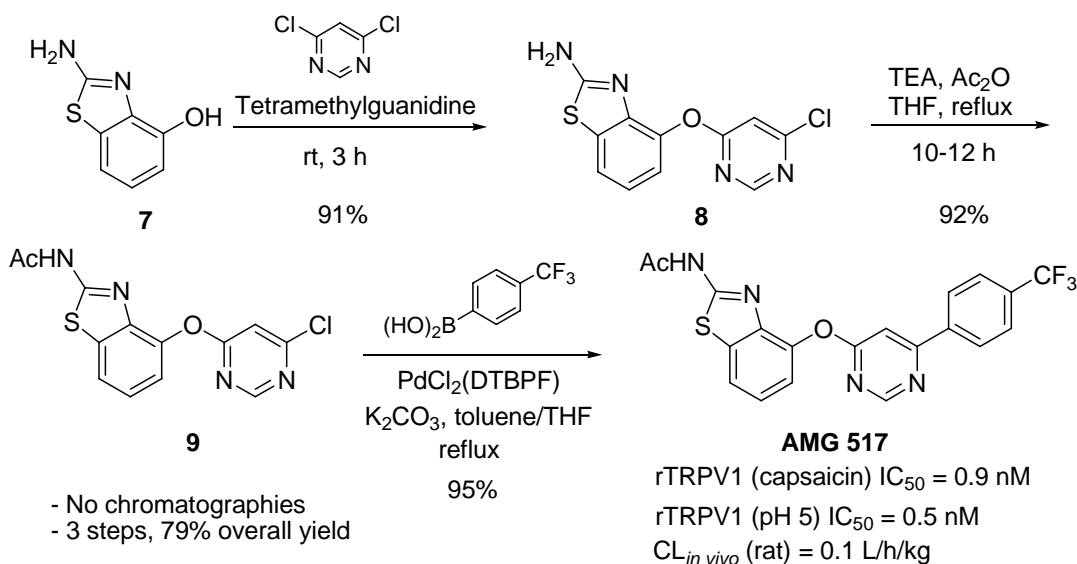


~ 70% of metabolism

Compound **5** was optimized further by varying the position of attachment of the quinoline ring; attachment to the 1-position was best, but resulted in a compound ineffective at blocking TRPV1 activation by a pH stimulus. Introduction of substituents on the quinoline ring was explored next, wherein the SAR revealed that compounds bearing an unsubstituted or monosubstituted amine were active versus both pH and capsaicin stimuli (Table 2). However, the best compound in this series, compound **6**,

underwent metabolism on the quinoline ring, with the O-sulfate formed accounting for ~70% of the observed metabolism. Hence, the quinoline ring was replaced by a benzothiazole, leading to AMG 517, the clinical candidate following optimization of the substituent on the benzothiazole ring. Approximately 25 kg of AMG 517 was prepared using the optimized process route shown below (Figure 2).

**Figure 2**



AMG 517 was shown to block activation of TRPV1 by capsaicin ( $IC_{50} = 0.8$  nM), pH 5 ( $IC_{50} = 0.6$  nM) and by heat ( $IC_{50} = 1.3$  nM). PK profiling (Table 3) revealed that the compound had good oral bioavailability, low clearance and linear dose response, with a long half life 31 hours in rat, 41 hours in dog and 62 hours in monkey.

**Table 3**

Species	Intravenous Dosing				Oral dosing
	$AUC_{0-inf}$ (ng.hr/mL)	CL (mL/hr/kg)	$V_{ss}$ (mL/kg)	$t_{1/2}$ (h)	$F$ (%)
Rat	8800	120	4000	31	51
Dog	7400	140	7000	41	23
Monkey	37000	30	2300	62	52
Human (projected)		50	4500	60-120	

AMG 517 was then evaluated in a variety of in vivo models: (a) Capsaicin-induced flinching in rats – AMG 517 blocked flinching with an  $ED_{50}$  of 0.3 mg/kg; (b) CFA

model in rats (Pain model) – AMG 517 reversed thermal hyperalgesia in the CFA model in rats (MED 0.83 mg/kg); (c) AMG 517 reverses hypothermia induced by capsaicin in a dose-dependent manner. It also causes moderate hyperthermia (+ 1.5 °C). Therefore, it appears that AMG 517 is thermoregulatory.

Phase 1 clinical studies (Single Dose Escalation PK) are currently underway for AMG 517. Linear PK was observed following oral administration of AMG 517 to healthy volunteers (1 to 25 mg dose); the half-life was still high (~300 h).

#### References:

- Ognyanov, V. I., et al, *J. Med. Chem.* 2006, **49**, 3719-3742  
Doherty, E. M., et al, *J. Med. Chem.* 2005, **48**, 71-90  
Xi, N. et al, *Bioorg. Med. Chem. Lett.* 2005, **15**, 5211-5217  
Gavva, N. R. et al, *J. Pharmacol. Exp. Ther.* 2005, **313**, 474-484
- 

#### Poster: “Design and Asymmetric Synthesis of F-Piperidine Spirocycles as iNOS Selective Inhibitors,”

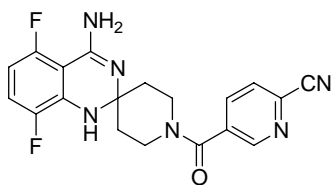
H. Yang,<sup>a</sup> C. Walpole,<sup>a</sup> Z. Liu,<sup>a</sup> F. Zhou,<sup>a</sup> N. Mackintosh,<sup>a</sup> S. Srivastava,<sup>a</sup> K. Carpenter,<sup>a</sup> J. Ducharme,<sup>a</sup> D. Menard,<sup>a</sup> M. N. Perkins,<sup>a</sup> A. Dray,<sup>a</sup> Allan Wallace,<sup>b</sup> Suzy Spriggs,<sup>b</sup> Anders Åberg,<sup>c</sup> Ernest Lee,<sup>d</sup> Robert Batey,<sup>d</sup>  
<sup>a</sup>AstraZeneca R&D Montréal, Canada; <sup>b</sup>AstraZeneca R&D Charnwood, UK;  
<sup>c</sup>AstraZeneca R&D Mölndal, Sweden; <sup>d</sup>Department of Chemistry, University of Toronto, Canada

Nitric oxide synthase (NOS) is an enzyme used by eukaryotes to synthesize NO from L-arginine. The NO synthesized thus functions as a messenger, and is involved in a variety of physiological functions. NOS exists as three different isoforms with diverse functions:

- (a) Neuronal or nNOS (Type I): constitutively expressed
  - regulation of learning and memory formation in brain
  - contributes to neurodegenerative disorders
- (b) Endothelial or eNOS (Type III): constitutively expressed
  - promotion of vascular relaxation
  - inhibition of platelet aggregation
- (c) Inducible or iNOS (Type II): induced by cytokines
  - contributes to various inflammatory diseases, including septic shock, RA, OA, asthma, ulcerative colitis, MS, and also to chronic pain

iNOS constitutes part of the host defense system, and is expressed in response to inflammatory cytokines. The NO produced then inactivates key metabolic enzymes in invading bacteria or tumor cells, which may lead to cell death or apoptosis. However, once activated, iNOS continues to be expressed for a long time, which may lead to overproduction of NO, and local cell damage. Thus, iNOS may play an important role in inflammatory processes.

Scientists at Astra Zeneca and the University of Toronto are engaged in the development of an orally active small molecule inhibitor of iNOS for the treatment of chronic pain.



**AR-C102222**

IC<sub>50</sub>(iNOS) = 42 nM

IC<sub>50</sub>(eNOS) = 92 μM

IC<sub>50</sub>(nNOS) = 1 μM

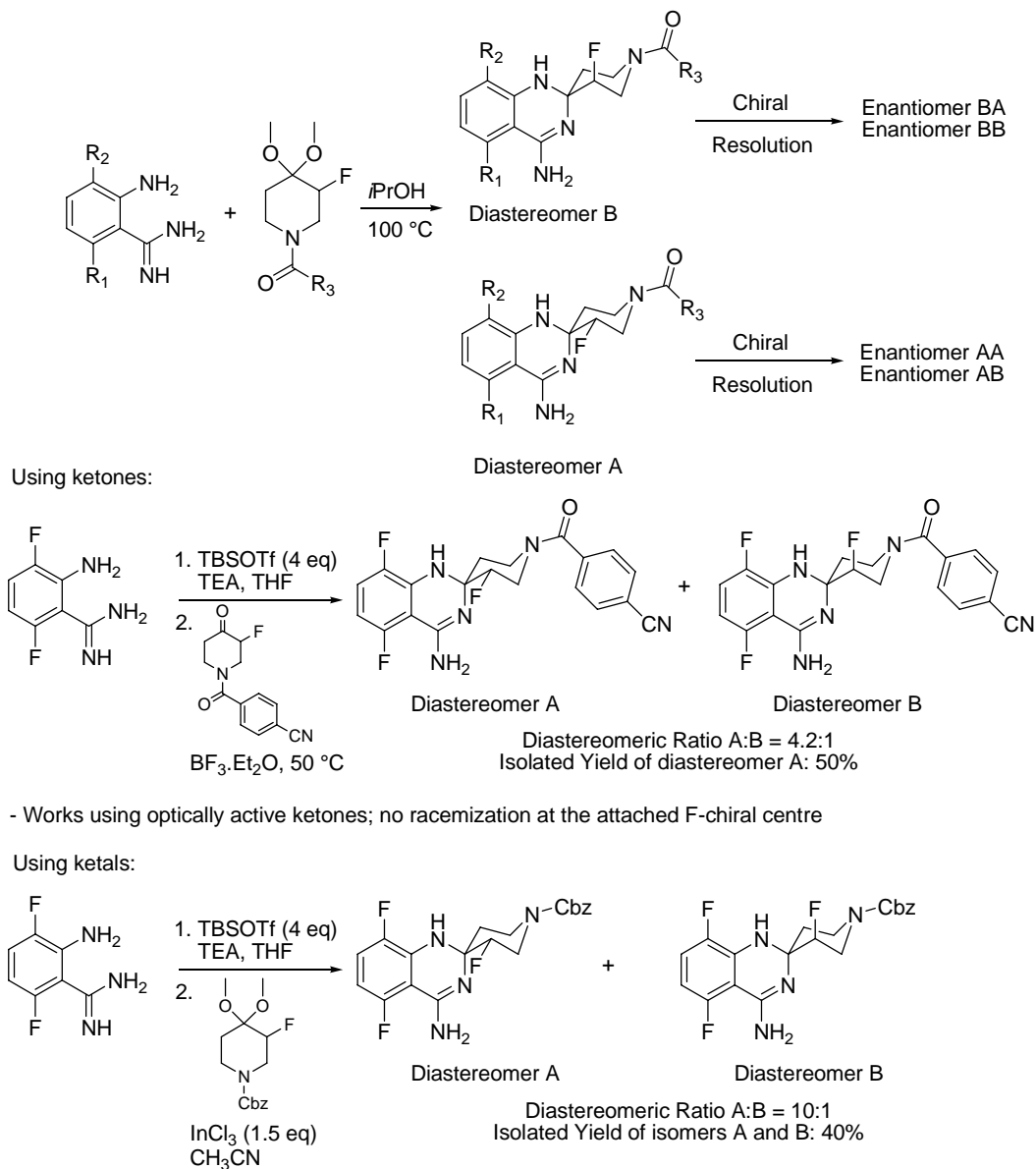
IC<sub>50</sub>(cell iNOS) = 1.3 μM

Their lead compound, AR-C102222, is competitive with L-arginine at the substrate binding site. The compound is a potent inhibitor of iNOS, with moderate to excellent selectivity over nNOS and eNOS respectively, and has demonstrated efficacy in various pain models. However, it does suffer for metabolic issues, including:

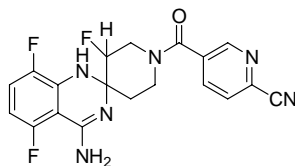
- (a) Displacement of 5-F on the aromatic ring by GSH
- (b) Amino cleavage
- (c) Reactive CN group on the pyridine ring (reacts with Cys/GSH)

The strategy pursued by these researchers involved introduction of fluorine atoms on the piperidine ring to improve metabolic stability and increase CNS/cell penetration. The added fluorine atom would help stabilize the amino group, increase the log D and reduce the pKa. The synthesis of the fluorinated spirocycles was achieved as shown in Figure 3. The diastereoselectivity of these reactions was improved by using various silyl triflates in the presence of Lewis Acids.

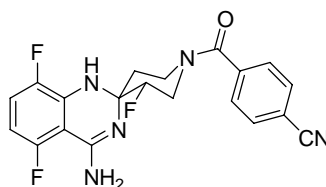
**Figure 3**



Of these fluorinated compounds, at least one of the two diastereomers retained biological activity, and showed improved pharmacokinetic properties (Table 4).

**Table 4**

				Rat PK, iv			
	R	Log D	pKa	Cl (L/h/kg)	Vdss (L/kg)	t <sub>1/2</sub> (h)	F (%), p. o.
Non-F parent	4-CNPh	0.82	8.16	5.70	3	0.4	<5
F-Isomer A	4-CNPh	1.35	7.60	1.32	1.1	1	41
F-Isomer B	4-CNPh	1.68	6.62	2.88	1.1	0.3	26
Non-F-parent	4-CN-3-Py	0.51	8.40	3.42	4.5	1.1	75
F-isomer A	4-CN-3-Py	0.92	7.74	2.04	2.2	1	41
F-isomer B	4-CN-3-Py	1.56	7.26	2.34	1.3	0.5	25

**AR-M102937**

$IC_{50}(iNOS) = 48 \text{ nM}$   
 $IC_{50}(eNOS) = \text{inactive}$   
 $IC_{50}(nNOS) = 25 \text{ } \mu\text{M}$   
 $IC_{50}(\text{cell } iNOS) = 4 \text{ } \mu\text{M}$

One fluorinated spirocycle, AR-M102937, was tested in the Bennett mouse (CCI) mechanical von Frey model (a neuropathic pain model). When dosed p.o. at 12.5  $\mu\text{mol/kg}$ , AR-M102937 almost completely reversed mechano-allodynia.

**References:**

Tinker, A. C. et al, *Curr. Top. Med. Chem.* **2006**, 6, 77-92

---

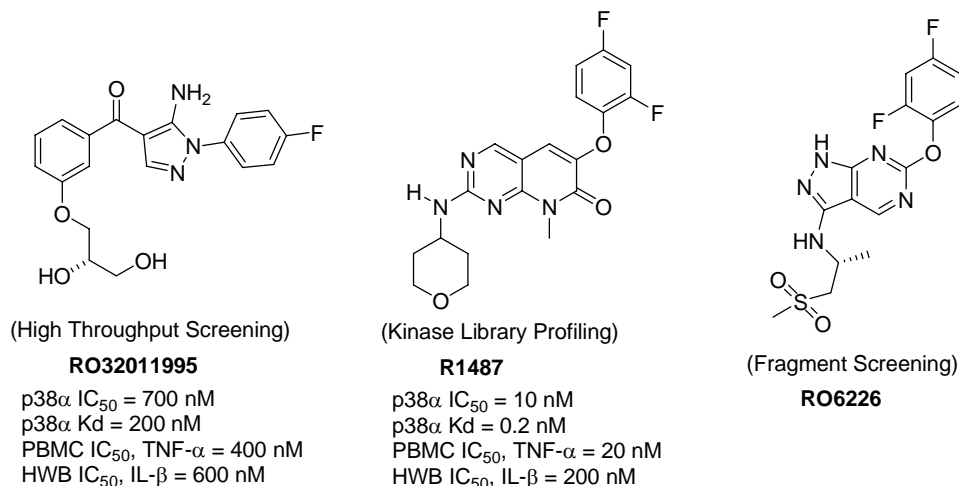
## Pathway to Clinic: “Inhibition of p38 MAP Kinase,”

Tobias Gabriel, Ph.D., (Roche) Palo Alto, CA

Dr. Gabriel described Roche’s approach toward the development of small molecule p38 inhibitors. Activation of p38 MAP kinase leads to increased biosynthesis of the proinflammatory cytokines TNF- $\alpha$  and IL-1 $\beta$ . Neutralization of TNF- $\alpha$  and IL-1 $\beta$  with biologic agents in clinical trials has been shown to lead to dramatic improvements in inflammatory diseases like RA, IBD and psoriasis. However, the prohibitive cost of such agents, coupled with inconvenient dosing regimens has reinforced the need for orally active, small molecule p38 inhibitors. Clinical trials with small molecule inhibitors have been hindered by safety issues, including hepatotoxicity, cardiotoxicity, CNS toxicity, skin rash, GI symptoms and infections.

A survey of the literature for p38 inhibitors undergoing clinical evaluation reveals compounds with a wide variety of chemotypes. An overview of various p38 chemotypes selected for development may be found in *Current Topic in Medicinal Chemistry*, **2005**, 5, 1017-1029 (Goldstein, D. M. et al). Roche scientists started out with multiple scaffolds in order to maximize their chances of success. These scaffolds were identified from diverse sources such as HTS, kinase library profiling, and fragment screening; the lead compounds resulting from three such scaffolds are shown below (Figure 4).

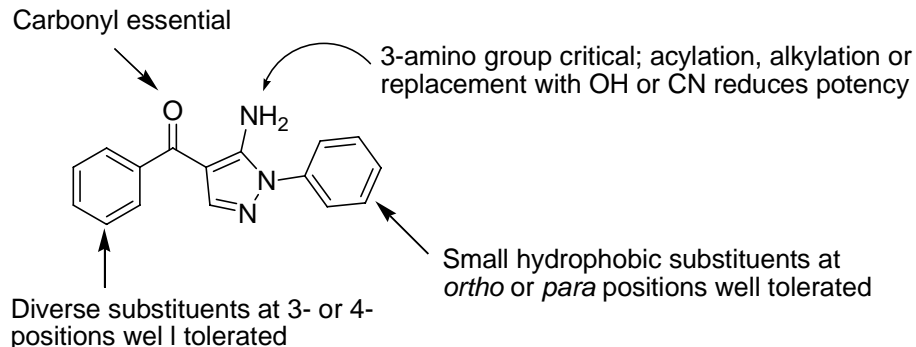
Figure 4



**Lead 1: RO3201195** (Reference: Goldstein, D. M. et al, *J. Med. Chem.* **2006**, 49, 1562-1575)

Several pyrazole ketones were identified via HTS, and optimized to give RO3201195. Initially, compounds in this series showed poor solubility and oral bioavailability. The chemists were guided by several co-crystal structures of compounds from this series in optimizing the physicochemical properties of the initial hit. The SAR for this series is summarized below (Figure 5).

**Figure 5**

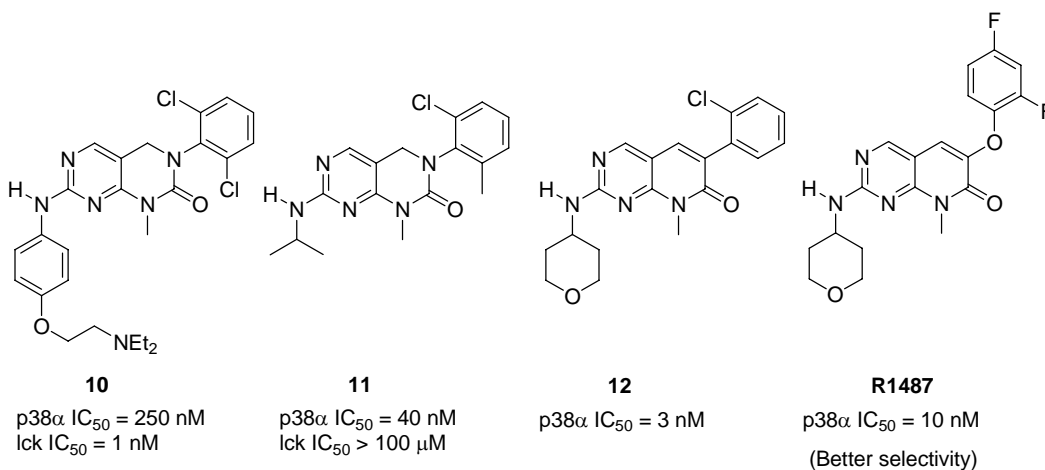


An X-ray crystal structure of RO3201195 bound to p38 $\alpha$  revealed a unique hydrogen bond between the amine of the inhibitor and threonine 106, unknown for previous p38 inhibitors. Threonine 106 is present in about 20% of human kinases, and therefore, the design of inhibitors with the capability of forming of a hydrogen bond to this residue should improve selectivity over other kinases lacking the residue. In addition, the pyrazole ketone forms a hydrogen bond to backbone NH of methionine 109 (this interaction is seen in all previously reported X-ray co-crystal structures of p38 inhibitors).

RO3201195 selectively inhibits p38, and was shown to inhibit the production of TNF- $\alpha$  and IL-1 $\beta$  in human whole blood. It was also effective at blocking the LPS-induced release of TNF- $\alpha$  and IL-6 in a rat *in vivo* model of acute inflammation. RO3201195 was subsequently evaluated in the clinic, where oral administration of the compound inhibited the *ex vivo* LPS-stimulated production of IL-1 $\beta$  in human whole blood, thus providing strong support for the continued evaluation of additional compounds for treatment of RA.

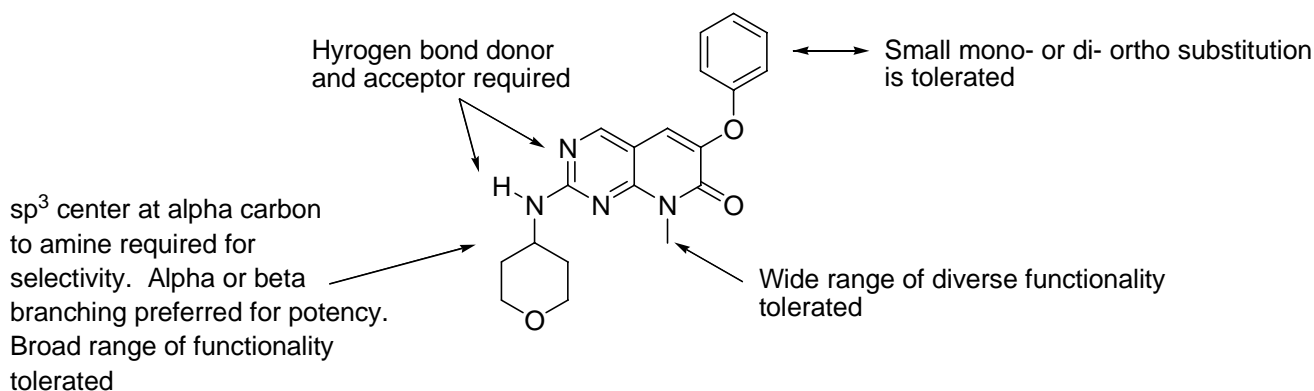
**Lead 2: R1487** (Reference: Goldstein, D. M. et al, *Current Topic in Medicinal Chemistry*, **2005**, 5, 1017-1029)

One of the hits from profiling of Roche's kinase library was compound **10**, which, in addition to showing affinity for p38, was also a potent inhibitor of p56<sup>lck</sup> (from the src kinase family). Both kinases had the requisite selectivity-conferring threonine residue.



Co-crystallization of compound **10** with both kinases revealed that the p38 binding pocket had a larger “front portion”. Filling in this extra space in the binding pocket by introducing a sp<sup>3</sup> carbon alpha to the exocyclic amine conferred selectivity for p38 over p56<sup>lck</sup> (compounds **11**, **12**, **R1487**). The SAR for this series leading to R1487 is summarized below (Figure 6).

**Figure 6**

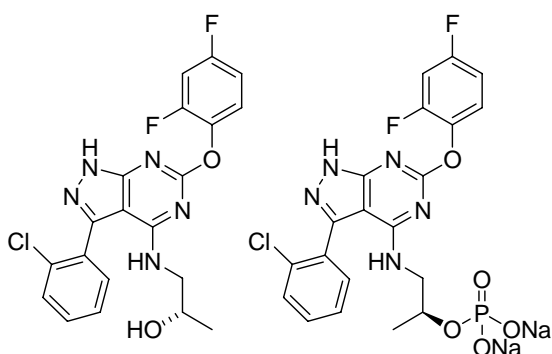


R1487 was found to be a selective p38 inhibitor *in vitro*, and was shown to inhibit the production of cytokines in human whole blood. It too was effective at blocking the LPS-induced release of TNF- $\alpha$  and IL-6 in a rat *in vivo* model of acute inflammation. R1487 was well tolerated in single oral doses (25 mg – 800 mg, suspension), and reduced *ex vivo* LPS-stimulated production of IL-1 $\beta$  in human whole blood.

**Lead 3: RO6226** A fragment screening approach was adopted in the quest for a backup compound belonging to a novel structural class with high selectivity (screening with Ambit

platform), potency in human blood <100 nM, and preclinical PK properties similar to R1487.

A specific kinase fragment library was compiled, and 20 Markush structures were selected. Both ACD and Roche libraries were searched, and 88 hits were identified. Fragment combination then led to the pyrazolopyrimidine lead series, exemplified by RO4499. This compound suffered from poor bioavailability, thought to be due to low solubility. The corresponding phosphate prodrug with much better solubility was prepared, but the oral bioavailability remained low. The PK data suggested high clearance, possibly via first pass metabolism (glucuronidation of parent) involving both liver and intestine. Indeed, the metabolism was found to be driven by the side chain.



**RO4499**

p38 $\alpha$  IC<sub>50</sub> = 6 nM  
 HWB IC<sub>50</sub> = 11 nM  
 Aq. Sol. 0.4  $\mu$ g/mL

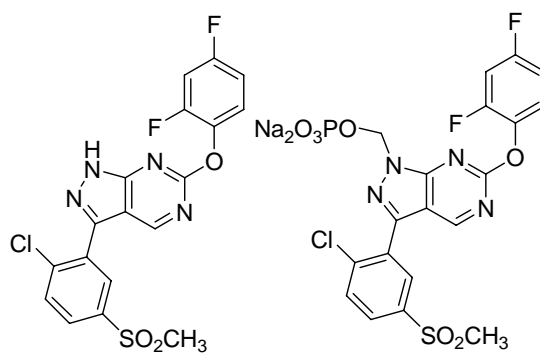
Monkey PK (3 mpk):  
 Cl = 15.6 mL/kg min  
 F = 0%

Rat LPS TNF inhibition:  
 41% @ 0.3 mpk  
 62% @ 3 mpk

**Prodrug of RO4499**

Aq. Sol. 6600  $\mu$ g/mL

Monkey PK (3.9 mpk):  
 F = 6%



**RO7125**

p38 $\alpha$  IC<sub>50</sub> = 0.00526  $\mu$ M  
 HWB IC<sub>50</sub>, IL- $\beta$  = 600 nM  
 Aq. Sol. 4.1  $\mu$ g/mL

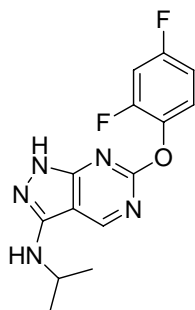
Rat LPS TNF inhibition:  
 72% @ 3 mpk

**RO3987**

Activated chloromethyl sulfone formed; cytotoxicity

Further optimization of the structure resulted in RO7125, which showed good stability in all liver and in vitro intestinal assays. The corresponding phosphate prodrug RO3987, showed vastly improved solubility and good oral bioavailability (47-69% F in rats, depending on formulation). However, the development of this compound was halted due to in vitro toxicity (related to formation of an activated chloromethyl sulfone; concentration-dependent loss in GSH levels in CHO-K1 cells and rat hepatocytes observed).

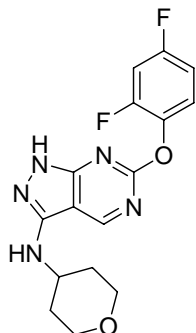
One other problem with the 3-phenyl pyrazolopyrimidines was their propensity for strong  $\pi$ -stacking and hydrogen bonding. Replacement of the 3-phenyl group with alkyl groups, ether, amides and amines eventually led to the identification of 3-amino pyrazolopyrimidines as potent p38 inhibitors.



**13**

p38 $\alpha$  IC<sub>50</sub> = 23 nM  
 HWB IC<sub>50</sub> = 21 nM  
 Aq. Sol. = 12  $\mu$ g/mL

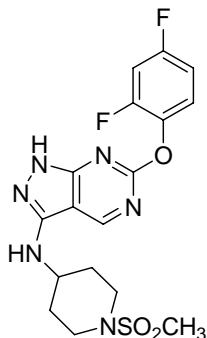
Low stability in hepatocytes



**14**

p38 $\alpha$  IC<sub>50</sub> = 73 nM  
 HWB IC<sub>50</sub> = 896 nM  
 Aq. Sol. = 77  $\mu$ g/mL

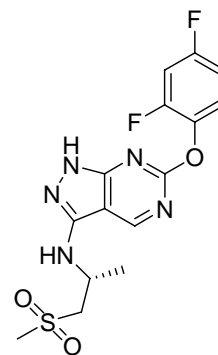
High stability in hepatocytes



**15**

p38 $\alpha$  IC<sub>50</sub> = 37 nM  
 HWB IC<sub>50</sub> = 125 nM  
 Aq. Sol. = 4  $\mu$ g/mL

High stability in hepatocytes



**RO6226**

p38 $\alpha$  IC<sub>50</sub> = 40 nM  
 HWB IC<sub>50</sub> = 39 nM  
 Aq. Sol. = 80  $\mu$ g/mL

High stability in hepatocytes

RO6226 is an extremely selective p38 inhibitor belonging to this series, with excellent physicochemical, pharmacological and ADME properties, which was then selected for preclinical development (Figure 7). Thus, the third Roche approach, based on fragment screening, with strong guidance from X-ray crystallography and modeling, resulted in a novel class of p38 inhibitors.

**Figure 7:**  
**RO6226 - ADME and Pharmacology**

*in vitro* ADME profile:

- Microsomal stability: High
- Hepatocyte stability: High
- No metabolites in RH and HH incubation assays
- P450 inhibition: human recombinant 1A2, 2C9, 2C19, 2D6, 3A4 > 50 mM

*in vivo* Pharmacology:

- Mouse LPS ED<sub>50</sub> = 0.3 mpk
- Rat LPS ED<sub>50</sub> = 1.5 mpk
- RO6226 inhibits collagen-induced arthritis in mice (73% reduction in disease scores at 90mpk)

*In vivo* ADME profile:

	<b>Rat</b>	<b>Monkey</b>
Dose (mpk)	3	3
Bioavailability	105%	62%
AUC <sub>0-inf</sub> ( $\mu$ g*h/mL)	1.22	5.85
C <sub>max</sub> ( $\mu$ g/mL)	0.446	0.597
Terminal t <sub>1/2</sub> (h)	3.70	2.37
Clearance (mL/min/kg)	43.6	5.47
V <sub>dss</sub> (L/kg)	8.10	1.10

---

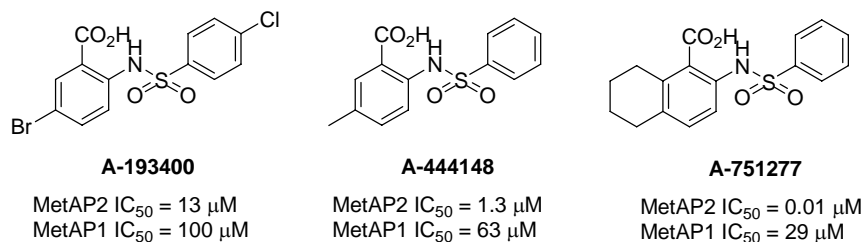
## “Discovery and Optimization of Anthranilic Acid Sulfonamides as Inhibitors of Methionine Aminopeptidase-2”

George S. Sheppard, Ph.D., Abbott Laboratories

Methionine aminopeptidases (MetAPs) remove methionine from the N-terminii of polypeptide chains, and are thought to play an important role in protein maturation. Of the three known human aminopeptidases (MeAP1, MetAP2, and MetAP-3/MetAP1D), MetAP2 is expressed in higher concentrations in tumors than in normal cells, where it appears to be essential for tumor growth and cell proliferation. MetAP2 was shown to be the molecular target of the anti-angiogenic agents fumagillin and TNP-470 (both are irreversible inhibitors, and alkylate a histidine residue on MetAP2). Further, fumagillin derivatives show anti-angiogenic activity in animal models.

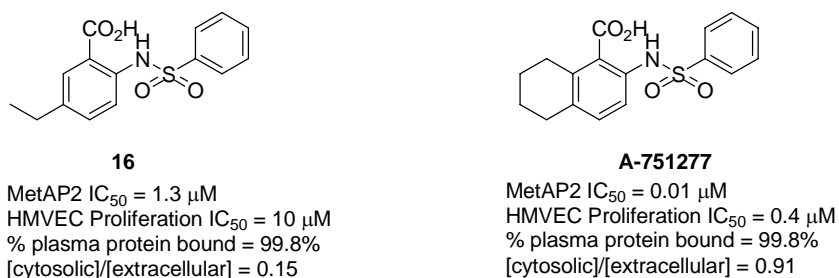
Affinity selection by mass spectrometry (ASMS) of  $Mn^{2+}$  MetAP2 was carried out in order to identify orally active, reversible, small molecule inhibitors. Several anthranilic acid sulfonamides were identified from the screen, and were shown to have oral bioavailability (Figure 8).

Figure 8



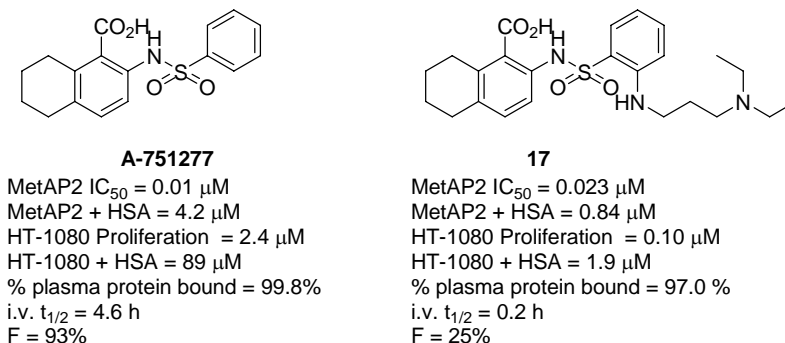
SAR of the initial analogues revealed potent inhibition of MetAP2 in vitro; however, only moderate activity was observed in a cellular assay. These analogues were found to be highly protein bound, and had poor permeability (Figure 9). Addition of human serum albumin (HSA, 40 mg/mL) produced significant drops in potency, indicating that binding to HSA were potentially problematic for this structural class.

Figure 9



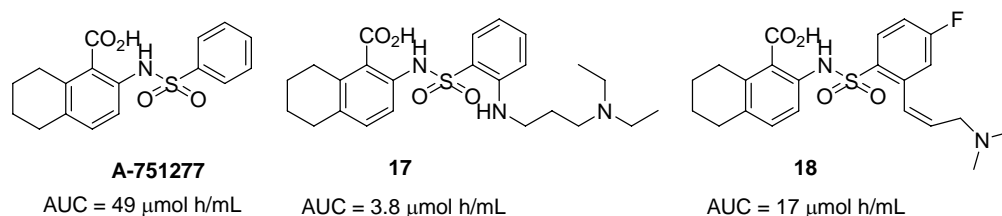
Comparison of a co-crystal structure of A-751277 bound to MetAP2 with an NMR structure of A-444148 bound to HSA suggested that ortho-substitution of the aryl sulfonamide would be accommodated by MetAP2 (where the substituent would be solvent exposed), but not by HSA (where the corresponding space is occupied by hydrophobic residues). Accordingly, a tethered amine substituent was introduced, and found to be tolerated (Figure 10).

**Figure 10**



Various core and tether variations were then prepared and evaluated in a serum shift assay. However, compounds with tethered amines had poorer PK properties, including diminished oral bioavailability. Further optimization of the tether led to the identification of Z-alkenyl analogues (Figure 11). Of these, one, A800141, showed good inhibition of tumor growth in the B16F10 model.

**Figure 11**



### References:

- Sheppard, G. S. et al, *J. Med. Chem.* **2006**, *49*, 3832-3849  
 Morowitz, M.J. et al, *Clin. Cancer Res.* **2005**, *11*, 2680-2685  
 Sheppard, G. S. et al, *Bioorg. Med. Chem. Lett.* **2004**, *14*, 865-868  
 Wang, J. et al, *Cancer Research* **2003**, *63*, 7861-7869